Coastal Engineering, 14 (1990) 457–477
Elsevier Science Publishers B.V., Amsterdam

A field study of wave reflections from an exposed dissipative beach

R.C. Nelson[a] and J. Gonsalves[b]
[a]*Department of Civil Engineering, University of New South Wales, University College, Australian Defence Force Academy, Campbell, A.C.T. 2600 (Australia)*
[b]*Division of Earth, Marine and Atmospheric Science and Technology, CSIR, Stellenbosch, (Republic of South Africa)*

(Received September 27, 1989; revised and accepted May 17, 1990)

ABSTRACT

Nelson, R.C. and Gonsalves, J., 1990. A field study of wave reflections from an exposed dissipative beach. *Coastal Eng.*, 14: 457–477.

This paper describes a field study of wave reflections from an exposed dissipative beach, using only water-surface elevation data from five wave height sensors. Many insights were gained into beach reflections and their detection. A technique normally reserved for laboratory use was successfully applied to surf zone data to separate incident and reflected infragravity wave-energy spectra. The reflected wave energy was found to be significant for all wave periods greater than 20 seconds, and often total for wave periods greater than 30 seconds. The evidence was heavily weighted towards the observed reflected wave activity being essentially two dimensional with the influence of three-dimensional edge waves being minimal. Other findings relate to the value of wave energy spectra computed from a single surf-zone sensor, the relevance of single slope approximations of beach profiles and the relationship between incident infragravity wave-activity and the longer-period swash excursions on a beach face.

1. INTRODUCTION

The surf zone is that region of the sea water environment where the wind wave energy is dissipated, mainly through wave breaking processes. The turbulence created also provides the mechanism by which sand particles are lifted above the bed to be transported by the prevailing currents. The magnitude and nature of this sediment movement varies with the incident wave action to change bed forms and improve the efficiency of the dissipation process. Masked by all this turbulent behaviour is another type of wave action, often referred to as surf beat, which occurs at infragravity frequencies, defined by Kinsman (1965) to correspond to a range of wave periods from about 30 seconds to 5 or 6 minutes. These waves are very long, shallow water waves with very small wave height to wave length ratios. They tend not to break, with the energy being reflected back off the beach, and during this process can

0378-3839/90/$03.50

provide the mechanism for the generation and maintenance of edge waves, a form of surf zone infragravity wave.

This infragravity wave action has important ramifications for coastal engineers. It affects water levels particularly at the beach face boundary. The currents they generate transport sand and influence the surf zone bathymetry. Infragravity waves will also have an important influence on the maximum wave heights that can be sustained in the wind wave frequency band. One of the primary factors governing whether any individual wave will or will not break, remain broken or reform into an oscillatory wave is the wave height to water depth ratio, known as the depth-limited wave height criterion. This is an important parameter in the selection of design wave heights in shallow water. The presence of infragravity oscillations underlying the waves at wind wave frequencies continually varies the effective water depth on which the wind waves are superimposed. Therefore, the maximum wave heights that can occur in the surf zone at wind wave frequencies will vary with time. These are just some of the reasons why it is essential for engineers to have an understanding of surf zone infragravity wave activity and the pitfalls inherent in its measurement.

Many field studies of surf zone behaviour have been undertaken. Some have concentrated on the wind wave spectrum, particularly the changes in nonlinearity, phase shifts, wave celerity and elementary ratios of characteristic wave

NOTATION

B_b	Galvin's onshore parameter ($=H_b/[gT^2\tan\beta]$)
C	wave celerity (phase velocity)
f	wave frequency
g	acceleration due to gravity
H_b	wave height at breaking
H_{mo}	spectral estimate of characteristic wave height ($=4\sqrt{m_0}$)
h	water depth
k	wave number ($=2\pi/L$)
L	wave length
m_0	zero moment of wave spectrum
m_1	first moment of wave spectrum
n_a	number of antinodes
n_n	number of nodes
S_i	spectral ordinates of incident wave spectrum
S_{ir}	spectral ordinates of combined incident and reflected wave spectrum
S_r	spectral ordinates of reflected wave spectrum
T	wave period
T_{m01}	spectral estimate of mean wave period ($=m_0/m_1$)
T_p	peak energy period
x	distance
β	beach slope
ϕ	phase shift
σ	angular velocity ($=2\pi/T$)

heights to mean water depth. These include, for example, Thornton et al. (1976), Suhayda and Pettigrew (1977) and Thornton and Guza (1982). Others have extended their studies to include infragravity frequencies including Hotta et al. (1981) and Wright et al. (1982). Important laboratory studies have also been undertaken. These include the studies of Guza and Bowen (1976) and Lin (1987/88). The studies acknowledge that in the presence of reflected infragravity waves, the analyses will exhibit energy distributions that are not indicative of the surf zone as a whole. They do not deal with the nature of these errors or the techniques that can be applied to isolate the true incident and reflected wave spectra.

This paper describes a field study which addresses these latter points and, in so doing, provides some valuable insights into beach reflections and their detection. The exercise described here is based on the collection of data from five wave height sensors spaced along a shore normal line between the beach face and a point outside the surf zone in 8 m of water. The study forms part of an overall programme which has as its aims the detection and nature of infragravity oscillations at the field study site, and the usefulness of data retrieved from various instruments deployed in the surf zone.

2. THE FIELD SITE AND EXPERIMENTAL SETUP

The field site was at Walker Bay, South Africa, located about 100 km south east of Cape Town (see Fig. 1). The beach has a total length of about 18 km and faces south west. This orientation, combined with offshore bathymetry of near-parallel offshore contours (see Fig. 2) normal to the prevailing southwesterly swells, ensures maximum exposure to waves which approach

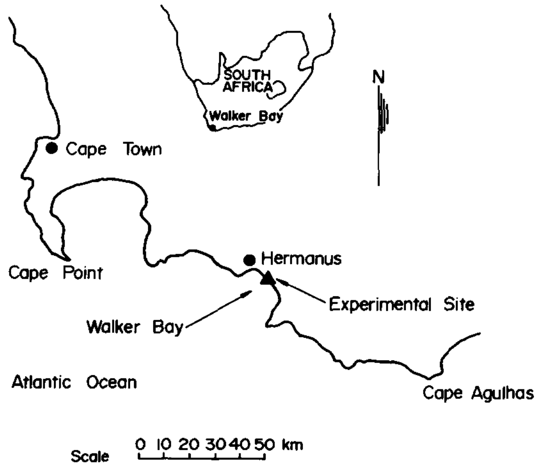

Fig. 1. Locality sketch.

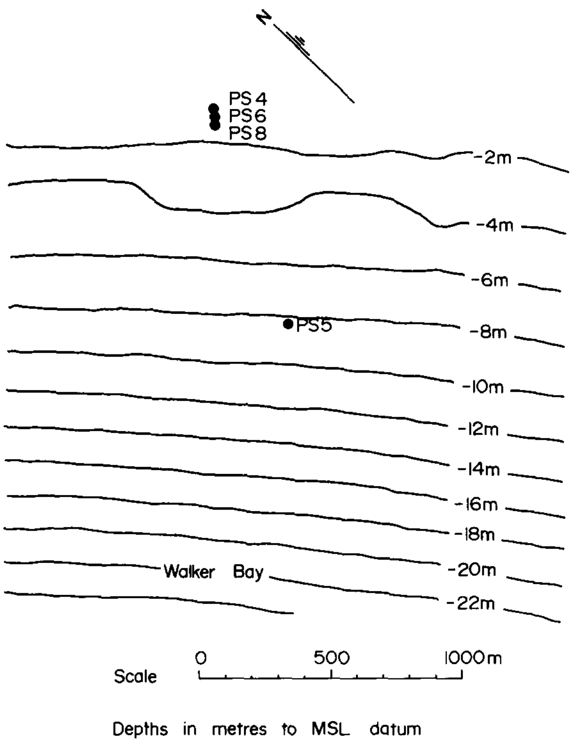

Fig. 2. Offshore bathymetry.

normal to the beach. Breaker heights in the area exceed 2 to 3 m most of the time with peak energy periods of about 12 s. The mean spring tide range is about 1.4 m with a mean neap tide range of 0.5 m. The median diameter of the beach sand varied between 0.35 and 0.55 mm. Surf zone widths in excess of 500 m are not uncommon at this site. The surf zone can be described as high energy and dissipative. Galvin (1972) empirically developed Eq. 1 as the criterion for spilling breakers:

$$B_b = \frac{H_b}{gT^2 \tan\beta} \geq 0.068 \tag{1}$$

For the site with $H_b \approx 2$–3 m, $T \approx 12$ s and $\tan\beta \approx 0.01$ the value of B_b is between 0.14 and 0.21, values which confirm visual assessments that the dominant beach forming wave characteristics are those of spilling breakers.

The instrumentation used in the experiment consisted of four pressure recorders fixed near the bed on steel supports, together with one resistance wire, wave runup meter located on the beach face. The pressure recorders used Schaevitz strain gauge pressure transducers with high accuracy and temperature stability. The recorders were attached to steel poles which were jetted into the sand, the transducers being finally located about 0.4 m above the bed.

All pressure recorders contained their own internal power source and programmable data logging mechanisms. One pressure recorder (PS5) was located outside the surf zone near the 8 m contour about 800 m from the beach face (see Fig. 2). Three pressure recorders were located inside the surf zone in a line normal to the beach (see Fig. 3). The innermost instrument (PS4) averaged about 53 m distance from the beach, defined as the intersection of the still water level and the beach profile. This distance varied with tide level. A second pressure recorder (PS6) was a further 36.6 m seaward with a third pressure recorder (PS8) a further 20.8 m seaward again. Observed mean water depths at PS6 varied between 1.5 and 2.5 m during the experiment. Depths at PS4 were about 0.2 m less than those at PS6 with those at PS8 being about 0.1 m deeper than those at PS6. The wave runup meter consisted of a resistance wire suspended 30–50 mm above the sand up the beach face. It was connected to a data logger similar to those used for the pressure recorders. The clocks on all five data loggers were synchronised and programmed to take simultaneous burst samples. The sample lengths used in this study consisted of 8192 readings at intervals of 0.5 s. The instruments were programmed so that the burst samples coincided with high and low water to minimise the influence of the astronomical tide on the record.

Data were actually collected over a period of seven days but instrument PS4 ceased to operate after five days. Maintaining satisfactory operation of the runup meter was a continual problem. The wire was often shorted out by

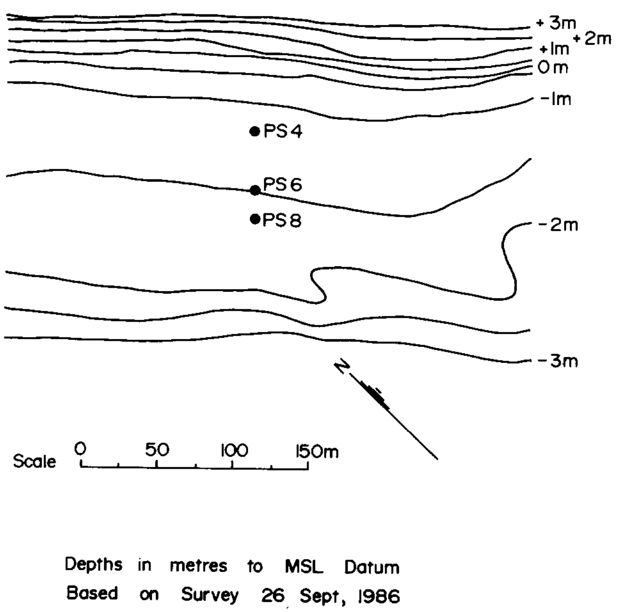

Fig. 3. Inshore bathymetry.

TABLE 1

Summary of wave conditions (September 1986)
(Based on all frequencies > 0.04 Hz; no. readings = 8192; $\Delta t = 0.5$ s)

Event	Start time		Mean depth	PS5		PS8		PS6		PS4	
	day	time (h)	at PS6 (m)	H_{mo} (m)	T_p (s)	H_{mo} (m)	T_p (s)	H_{mo} (m)	T_p (s)	H_{mo} (m)	T_p (s)
1	22	1556	2.54	1.92	12.5	1.20	14.3	1.02	15.4	0.76	15.4
2	22	2203	1.53	1.92	12.5	0.71	15.4	0.57	15.4	0.43	18.2
3	23	0412	2.31	2.10	14.3	1.11	14.3	0.97	15.4	0.74	15.4
4	23	0959	1.65	2.75	14.3	0.77	20.0	0.63	18.2	0.46	18.2
5	23	1623	2.34	2.23	13.3	1.13	14.3	1.00	15.4	0.75	16.7
6	23	2233	1.57	1.82	13.3	0.73	14.3	0.61	14.3	0.42	18.2
7	24	0441	2.17	1.45	12.5	0.98	12.5	0.88	12.5	0.64	16.7
8	24	1029	1.65	1.31	11.8	0.73	12.5	0.62	13.3	0.43	18.2
9	24	1653	2.15	1.23	11.1	0.92	11.8	0.83	12.5	0.61	11.8
10	24	2309	1.59	1.30	11.1	0.64	11.8	0.54	11.8	0.39	18.2
11	25	0517	2.00	1.62	10.5	0.81	12.5	0.74	13.3	0.52	16.7
12	25	1108	1.64	1.62	11.8	0.66	16.7	0.59	16.7	0.44	18.2
13	25	1736	1.93	1.69	11.8	0.80	14.3	0.69	14.3	0.53	18.2
14	26	0007	1.55	1.63	13.3	0.68	16.7	0.58	20.0	0.44	18.2
15	26	0627	1.80	1.56	13.3	0.79	14.3	0.67	16.7	0.48	16.7
16	26	1309	1.64	1.09	12.5	0.67	13.3	0.56	13.3	0.42	18.2
17	26	1939	1.80	0.82	12.5	0.67	13.3	0.58	13.3	0.43	16.7

sand level changes, seaweed entanglements, people walking on the wire and motor vehicles running over the wire. As a result there are only three runup records that can be accepted as satisfactory. In the final analysis there are available 17 records where synchronous, simultaneous burst samples were taken from PS5, PS8, PS6 and PS4 and for three of which there are simultaneous records of wave runup.

A summary of the wind wave conditions experienced during the experiment is given in Table 1, together with the time of commencement of each burst sample. Relative water levels for each burst sample can be judged from the mean water depths given for PS6, the middle recorder in the array of three pressure recorders located in the surf zone. An event number has been assigned to each burst sample and it is this number that is used to identify each burst sample elsewhere in this paper.

3. REFLECTED INFRAGRAVITY WAVES AND THE MEASURED INFRAGRAVITY SPECTRUM

The presence of incident infragravity waves that are reflected back off a beach will create standing waves in the onshore–offshore direction. A wave energy spectrum, computed using data from a single wave height sensor located in the surf zone, may then exhibit distributions of infragravity energy that are not indicative of the surf zone as a whole and which can be misleading as to the total infragravity energy present in the general surf zone. These aspects can best be understood by considering the following simple model.

Consider a spectrum of linear shallow water waves such that the energy is equally distributed at all frequencies, as shown in Fig. 4a. That is, the energy density is a constant value at all frequencies and is equal to a value S_i. Assume this wave spectrum propagates over water of constant depth to be incident normal to a vertical wall from which it is totally reflected (see Fig. 4b). It can then be shown that the measured distribution of the wave energy detected by a single wave height sensor would be as shown in the nondimensional plot of

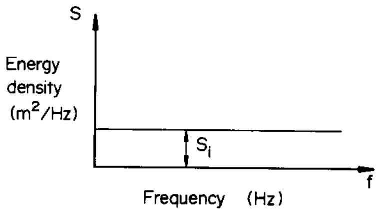

(a) Incident Wave Spectra for Schematic Model

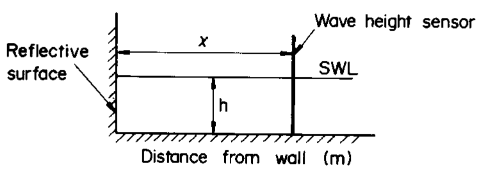

(b) Schematic Model

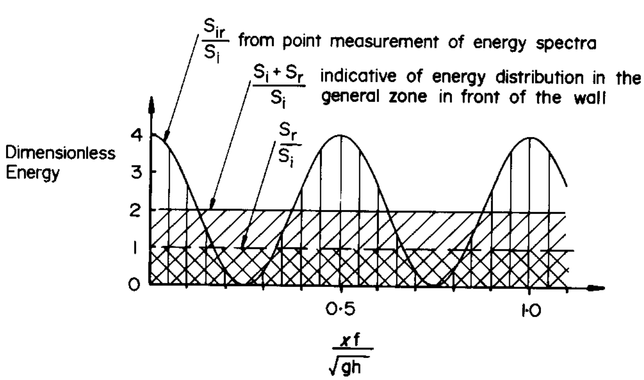

(c) Spectra Comparisons

Fig. 4. Measured and true standing wave spectra (single sensor) using a simple model.

Fig. 4c, where S_{ir} represents the spectral ordinates obtained from a single point measurement in the zone containing both incident and reflected energy spectra. The equation of the measured energy distribution is as given by Eq. 2:

$$\frac{S_{ir}}{S_i}=4\cos^2\left(\frac{2\pi xf}{\sqrt{gh}}\right) \tag{2}$$

This clearly shows troughs in the spectrum at those frequencies for which nodes will form at a given location x and peaks at those frequencies for which antinodes will form at a given location x. The frequencies associated with the nodes and antinodes are those given by Eqs. 3 and 4.

For nodes:

$$f=\frac{[2n_n-1]\sqrt{gh}}{4x} \tag{3}$$

where $n=1, 2, 3$, etc., and is the number of nodes present between the reflective surface and the location x, including the one at x.

For antinodes:

$$f=\frac{[n_a-1]\sqrt{gh}}{4x} \tag{4}$$

where $n=1, 2, 3$, etc., and is the number of antinodes that exist between the reflective surface and the location x, including the one at the reflective surface and the one at x. The energy distribution more indicative of the general zone in front of the wall is that described by Eq. 5 and also shown in Fig. 4c:

$$\frac{S_i+S_r}{S_i}=2 \tag{5}$$

This does not have the troughs and peaks exhibited in the measured data. However, it can also be seen that, provided a sufficiently wide band of frequencies is considered, the total energy in this spectrum will equal that in the measured spectrum such that spectral estimates of wave height (H_{mo}), obtained from each spectrum, will be the same. The distribution of wave energy in the measured spectrum is also such that, provided a sufficiently wide band of frequencies is considered, then spectral estimates of mean wave period (T_{m01}) obtained from each spectrum will be the same.

Figure 4c also demonstrates the effect of incident wave spectra where the energy exists only over a finite band of frequencies. If that band width coincides with a peak in Eq. 2, then the measured spectrum will overestimate the general energy level contained by the zone in front of the wall. If the band width coincides with a trough in Eq. 2, then the measured spectrum will underestimate the general energy level contained by the same zone. If the band width becomes sufficiently narrow, the ratio of the energy in the measured spectrum to the actual level indicative of the general zone in front of the wall, can be between a value approaching zero and a value approaching 2.

The above simple model makes it clear that in real surf zones containing a reasonably broad band of standing infragravity wave frequencies, measured wave spectra from a single sensor will exhibit troughs at those frequencies associated with nodes at the station and peaks at those frequencies associated with antinodes at the station. However, the fact that there are standing waves cannot be deduced solely from the data from one station, as it is possible that low and high energy frequencies exist. The analysis of data from several stations spaced normal to the shore, can assist in delineating between the two possibilities. A shift in the frequencies at which peak and trough energies occur at each station, betrays the existence of standing waves. The existence of low energy levels at frequencies quite active at a nearby station does not convey a reasonable assessment of general surf zone energy levels.

An example of this phenomenon is shown in Fig. 5 which shows the measured wave spectra at stations PS8, PS6 and PS4 for event number 1 in Table 1. The peak and trough energy levels at each station occur at different frequencies. The frequencies at which they occur is increased the closer the sensors are located to the shore line, indicating the shorter wave lengths required for nodal and antinodal distances to match the reducing distance between the beach face and the wave sensor.

To sum up, it can be stated that a single surf-zone wave height sensor cannot conclusively detect the presence of infragravity standing waves. However, if they are present, troughs and peaks will occur in the measured spectrum which are not indicative of energy levels in the surf zone as a whole. Again, if

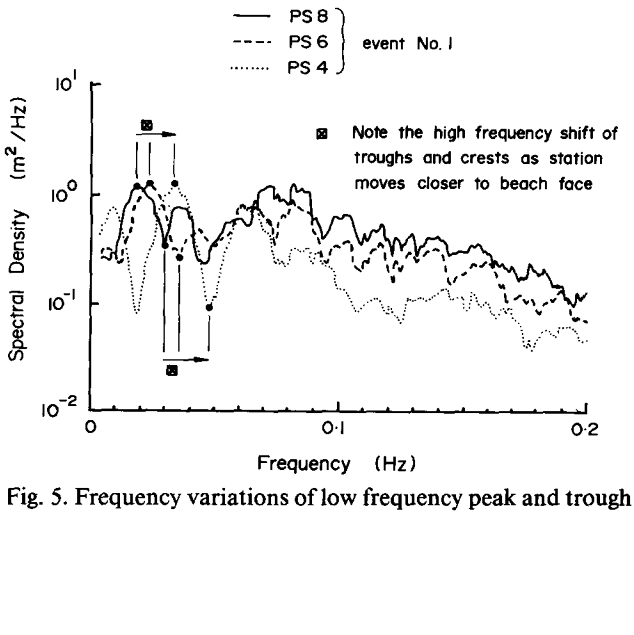

Fig. 5. Frequency variations of low frequency peak and trough energies.

they are present, the measured spectrum may overestimate or underestimate the total infragravity wave energy present in the surf zone depending on water depth, distance from the beach and the range of frequencies over which the energy is spread. Because water depth and distance from the beach varies with tide level it is conceivable that the degree of error will vary with the tidal variations. The infragravity peak energy periods determined from a single surf-zone wave height sensor have no real meaning for the surf zone as a whole if standing wave energy is present.

4. SEPARATION OF INCIDENT AND REFLECTED LONG WAVE ENERGY

The considerations of Section 3 above indicates that if data from wave height sensors only is available, the data from more than one location will be required to separate incident and reflected infragravity wave energy. The method used in this experiment was that of Mansard and Funke (1980). This requires the simultaneous measurement of water level variation with time at three positions located along a line parallel to the direction of the incident and reflected wave propagation. The method assumes that the wave motion is approximately linear in character. Therefore, in the surf zone it cannot be applied at wind wave frequencies, where waves are broken or breaking and are highly nonlinear. The method can, however, be applied to that part of the spectrum where the waves have low heights and long lengths and which are most likely to reach the beach unbroken and be reflected back in the seaward direction, namely the infragravity wave energy.

Data from stations PS8, PS6 and PS4 were used in this experiment. The spacing of the three pressure sensors fitted the application requirements adequately. The analyses were undertaken over three frequency band-widths nominally matching the wave period band widths of 20–30 s, 30–60 s and 1–6 min. The results are shown in Tables 2, 3 and 4. Overall the results show a trend of decreasing reflectivity with increasing wave frequency and on average indicate the following reflection coefficients and standard deviations over the 17 events analysed.

20–30 s: 53% ± 15%

30–60 s: 81% ± 20%

1–6 min: 92% ± 14%

However, it will be observed from Fig. 6 that water level has a large influence on both the average magnitude of the reflection coefficients and the data scatter. Reanalysis of the data for high and low water conditions gave the following results for means and standard deviations.

TABLE 2

Incident and reflected wave energy spectra
($20\ s < T < 30\ s$; no. readings$=8192$; $\Delta t=0.5\ s$)

Event	Incident spectra		Reflected spectra		Reflection coeff. (%)
	H_{mo} (m)	T_{m01} (s)	H_{mo} (m)	T_{m01} (s)	
1	0.30	25	0.16	25	53
2	0.26	25	0.06	26	23
3	0.31	25	0.20	25	64
4	0.25	24	0.09	24	34
5	0.28	24	0.14	26	51
6	0.22	24	0.08	24	37
7	0.22	25	0.13	25	58
8	0.18	25	0.08	24	47
9	0.19	24	0.11	25	57
10	0.15	25	0.08	25	54
11	0.19	25	0.11	24	57
12	0.23	25	0.11	23	49
13	0.26	25	0.14	25	53
14	0.26	25	0.11	24	41
15	0.22	25	0.13	25	61
16	0.16	24	0.12	24	77
17	0.11	25	0.09	24	86

TABLE 3

Incident and reflected wave energy spectra
($30\ s < T < 60\ s$; no. readings$=8192$; $\Delta t=0.5\ s$)

Event	Incident spectra		Reflected spectra		Reflection coeff. (%)
	H_{mo} (m)	T_{m01} (s)	H_{mo} (m)	T_{m01} (s)	
1	0.33	39	0.30	44	91
2	0.33	42	0.11	47	34
3	0.37	42	0.29	46	79
4	0.31	40	0.21	47	69
5	0.29	43	0.28	42	94
6	0.27	41	0.14	45	52
7	0.24	40	0.22	47	91
8	0.29	41	0.17	45	60
9	0.21	41	0.18	45	85
10	0.19	40	0.12	43	63
11	0.27	42	0.28	50	102
12	0.29	42	0.22	47	76
13	0.32	40	0.31	48	97
14	0.29	41	0.19	48	65
15	0.27	39	0.26	47	95
16	0.22	44	0.24	48	110
17	0.18	41	0.20	45	111

TABLE 4

Incident and reflected wave energy spectra
(1 min < T < 6 min; no. readings = 8192; Δt = 0.5 s)

Event	Incident spectra		Reflected spectra		Reflection coeff. (%)
	H_{mo} (m)	T_{m01} (s)	H_{mo} (m)	T_{m01} (s)	
1	0.32	85	0.27	87	84
2	0.35	100	0.24	112	67
3	0.35	94	0.31	101	87
4	0.36	90	0.32	104	90
5	0.38	82	0.34	95	91
6	0.33	90	0.24	104	72
7	0.25	92	0.21	95	87
8	0.28	88	0.18	97	66
9	0.18	81	0.18	85	96
10	0.20	87	0.21	89	102
11	0.28	85	0.33	94	118
12	0.33	93	0.31	100	93
13	0.32	86	0.34	94	107
14	0.44	100	0.41	111	94
15	0.37	93	0.36	99	100
16	0.27	91	0.27	93	98
17	0.20	87	0.22	93	109

High water:	20–30 s:	60% ± 11%
	30–60 s:	94% ± 9%
	1–6 min:	98% ± 12%
Low water:	20–30 s:	45% ± 16%
	30–60 s:	66% ± 22%
	1–6 min:	85% ± 15%

The results show a consistent trend toward much larger reflection coefficients at high water than at low water with a greater variability in the values observed at low water. No definitive explanation can be offered for this behaviour although some possible mechanisms can be suggested. Perhaps the availability of the steeper beach face at high tide (see Fig. 8) provides a more concentrated reflective surface. Perhaps the greater surf zone widths at low water, and hence the greater turbulence generated by the superimposed broken and breaking waves, suppresses the reflected waves in much the same way as Guza and Bowen (1976) observed for edge waves.

The overall variability in the data will be in part real but some will be due to errors in the procedure used to separate the incident and reflected wave spectra. How much is attributed to each is not possible to discern, but it is certain that reflection coefficients greater than 100% are not possible, yet some such values were obtained. These may give some guidance to the accuracy of the analysis technique. For example, from the results for high water in the 1–6 min wave-period band (98% ± 12%) one can speculate that the error in the analysis is about 10% because reflection coefficients greater than 100% are not possible.

The results demonstrate that wave reflection is significant for all wave periods greater than 20 s and that the reflection can be total at most wave periods greater than 30 s.

It will be seen in Tables 2, 3 and 4 that the wave heights have been rounded off to two decimal places. The reflection coefficients were based on wave height estimates that were not rounded off and therefore the tabulated values may vary slightly from a ratio based on wave heights given in the tables.

5. INFRAGRAVITY SWASH

The analyses of incident and reflected wave spectra at infragravity frequencies clearly indicates significant wave reflection at wave periods greater than 30 s. This would have created standing waves in the onshore–offshore direction with the first antinode at the beach face. The vertical water movements at this antinode, and their relationship to infragravity oscillations elsewhere in the surf zone, can be estimated from the runup meter data. These data were converted to equivalent vertical water movements, knowing the resistance characteristics of the wire and the beach profile along which it was laid. Only three data sets are available (see Section 2). These were analysed over the 30–60 s wave period band and over the 1–6 min wave period band. The results are summarised in Table 5. Three values of the ratio $H_{\mathrm{mo(swash)}}/H_{\mathrm{mo(incident)}}$ are given. The first and higher value is based on an incident H_{mo} value obtained directly from the analysis separating incident and reflected wave spectra (i.e., from Tables 3 and 4). This value takes no account of the shoaling effects on the infragravity waves as they traverse the distance between the pressure sensors and the beach face. When this correction is made, then those values shown for 1.0 m and 0.5 m depths apply. The lower ratio values for event 12 may well be due to the tide level being in that range which produced lower reflection coefficients (see Tables 1, 3 and 4 and Fig. 6).

The results fit a model where there are onshore–offshore standing waves with an antinode at the beach face. When there is near total reflection, the maximum vertical movements at this antinode are about twice those of the incoming long wave phenomenon. For practical purposes it seems some quantitative knowledge of surf zone infragravity wave activity can be gained

TABLE 5

Results of swash analysis
(No. readings = 8192; Δt = 0.5 s)

Period band	Event	Incident wave spectra				Vertical swash		$H_{mo(swash)}/H_{mo(incident)}$		
		No shoaling correction		Shoaled to 1 m	Shoaled to 0.5 m			No correction	Corrected to 1 m	Corrected to 0.5 m
		H_{mo} (m)	T_{m01} (s)	H_{mo} (m)	H_{mo} (m)	H_{mo} (m)	T_{m01} (s)			
30 s	12	0.29	42	0.32	0.39	0.59	41	2.06	1.82	1.53
to	13	0.32	40	0.37	0.44	0.87	41	2.75	2.33	1.97
60 s	16	0.22	44	0.24	0.29	0.62	44	2.88	2.55	2.15
1 min	12	0.33	93	0.37	0.44	0.71	95	2.15	1.90	1.60
to	13	0.32	86	0.37	0.44	0.90	90	2.86	2.42	2.04
6 min	16	0.27	91	0.31	0.36	0.74	95	2.72	2.41	2.04

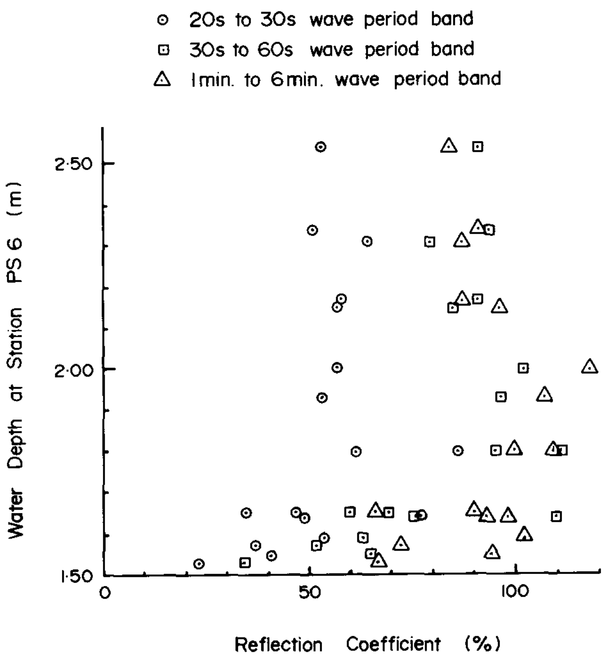

Fig. 6. Reflection coefficient versus water depth.

by simple observations of the longer period swash excursions on the beach face.

6. REFLECTED INFRAGRAVITY WAVES AND THE PHASE SHIFT SPECTRUM

Phase shift spectra between two surf zone stations aligned parallel to the wave direction, are a useful tool for gaining insights into surf zone behaviour. They are, for example an essential part of the process by which incident and reflected wave spectra were separated from measured wave data in Section 4. They are also a useful tool for estimating wave celerities in the surf zone at given frequencies. Thornton et al. (1976) has shown that if two wave sensors are spaced Δx apart in a line parallel to the direction of wave propagation, then a spectral component characterised by a frequency σ will have a phase shift ϕ between the two sensors as given by Eq. 6:

$$\phi_\sigma = k_\sigma \Delta x = \frac{\sigma \Delta x}{C} \tag{6}$$

If the phase shift is known, the celerity can be estimated from the same equation. Where the phase shift spectrum is a straight line passing through zero, as is often the case in a surf zone, it is indicative of progressive waves in a nondispersive system where the waves at all frequencies have the same celerity.

However, the phase shift spectrum should also indicate the presence of standing waves by detecting the existence of nodes and enable the frequency associated with those nodes to be determined. The reasoning is that if a node for a particular frequency lies seaward or shoreward of both wave sensors, then the vertical water movements at both instruments are in phase and would exhibit zero phase shift at that frequency under ideal conditions. If a node falls between the two sensors, the vertical water movements at both sensors are out of phase at that frequency and would exhibit maximum phase shift at that frequency. Under ideal reflective conditions this phase shift would be 180°, but this will not be achieved in practice due to factors such as smoothing operations in the computational procedures and because reflections may only be partial. One would also expect the peaks in the phase shift spectrum to occur at lower frequencies for low tide conditions than they do at high tide for the following reason. Assuming the reflective surface is a fixed distance from the observation stations, then as the wave length at a given frequency reduces in shallower water, a lower frequency (longer wave length) is required to achieve the wave length necessary for the node location to match the fixed distance between the wave sensors and the reflective surface.

Figure 7 shows the phase shift spectra between stations PS8 and PS6 for the first three data sets collected during the field experiment. They exhibit all the characteristics described above. Reflective activity can be seen to have a very strong influence up to the peak wave energy frequency after which the

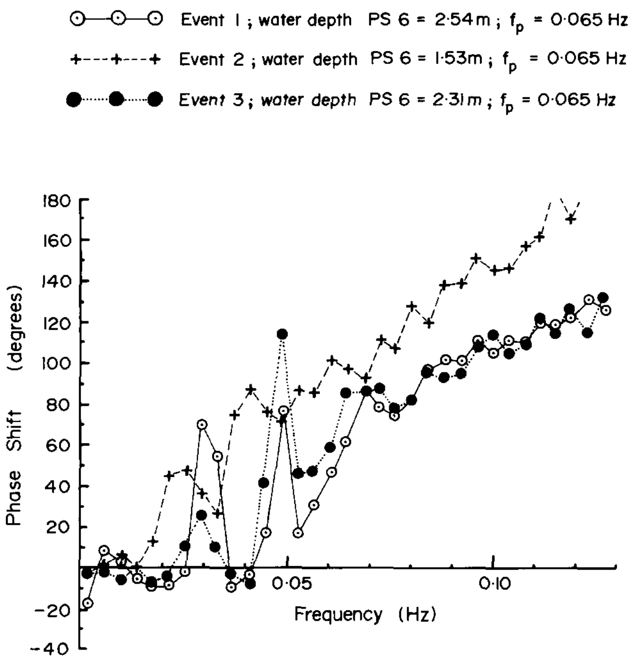

Fig. 7. Typical phase shift spectra between PS8 and PS6.

waves become progressive and nondispersive. The peaks in the phase shift spectra at low frequencies are indicative of those frequencies for which nodes are falling between the wave sensing stations. These three phase shift spectra exhibit two strong nodal frequencies, as did all 17 data sets. There is a trend toward zero phase shift before and in between these nodal frequencies. The frequencies at which these nodes occurred for all data sets are shown in Table 6 and are designated f_2 and f_3. They are respectively those frequencies for which the distance to the second node $(3L_2/4)$ and the third node $(5L_3/4)$ match the distance between the effective reflective surface and the wave sensors. The table clearly demonstrates the downward and upward shift of the nodal frequencies with alternate low and high water levels respectively.

There is actually a third nodal frequency (f_1) in all data sets at a frequency lower than both those shown in Table 6. It was very weakly evident in some of the phase spectra at about 0.01 Hz (see for example Fig. 7). Part of the explanation for the indefinite character of this phase shift peak is the computational smoothing used in banding the spectra. At low frequencies the spectral frequency banding width will always be greater relative to the range of frequencies that can form nodes over the length between the wave sensors, than it is at higher frequencies. There is a greater tendency, therefore, to "iron out" the low frequency phase shift peaks. However, this is not the only explanation because attempts to minimise the effects of smoothing only produced

TABLE 6

Observed and predicted nodal frequencies
(Observed frequencies from phase shift spectra between PS8 and PS6 – predicted frequencies after Hotta et al. (1981) using a compound two slope beach)

Event	Depth PS6 (m)	x (Fig. 4) (m)	Observed nodal frequencies f_1 (Hz)	f_2 (Hz)	f_3 (Hz)	Predicted nodal frequencies f_1 (Hz)	f_2 (Hz)	f_3 (Hz)
1	2.54	113		0.0293	0.0488	0.0102	0.0250	0.0400
2	1.53	96		0.0254	0.0410	0.0100	0.0263	0.0400
3	2.31	107		0.0293	0.0488	0.0102	0.0256	0.0400
4	1.65	97		0.0254	0.0449	0.0103	0.0263	0.0400
5	2.34	108		0.0293	0.0527	0.0103	0.0256	0.0400
6	1.57	96		0.0254	0.0410	0.0103	0.0263	0.0400
7	2.17	109		0.0293	0.0488	0.0104	0.0256	0.0400
8	1.65	97		0.0254	0.0410	0.0103	0.0263	0.0400
9	2.15	108		0.0293	0.0488	0.0104	0.0256	0.0400
10	1.59	97		0.0254	0.0371	0.0100	0.0263	0.0400
11	2.00	100		0.0293	0.0410	0.0103	0.0256	0.0400
12	1.64	97		0.0254	0.0449	0.0100	0.0263	0.0400
13	1.93	99		0.0293	0.0449	0.0102	0.0263	0.0400
14	1.55	96		0.0254	0.0449	0.0100	0.0263	0.0400
15	1.80	98		0.0293	0.0410	0.0102	0.0263	0.0400
16	1.64	97		0.0254	0.0410	0.0103	0.0263	0.0400
17	1.80	98		0.0293	0.0449	0.0102	0.0263	0.0400
Overall means (Hz)			≈0.0100	0.0275	0.0444	0.0102	0.0260	0.0400
Frequency range (Hz) allowing for sensor spacing each side of mid location						±0.0014	±0.0021	±0.0033

marginally better results. These lower frequency nodes may have been unstable with respect to location and wandered in and out of the region between the sensors.

7. OBSERVED NODAL FREQUENCIES VERSUS THEORETICAL PREDICTIONS

Hotta et al. (1981) published theoretical solutions for standing waves on single slope beaches and on compound beaches consisting of two slopes. These models were applied to the Walker Bay field site and the results compared with the observed values of nodal frequencies obtained from the phase shift spectra. The beach profile for the site is shown in Fig. 8. A compound two slope model with the slopes shown in the figure, fits this profile well. The mid point between stations PS8 and PS6 was adopted as the fixed location of the observation point. The distance x between this point and the beach face then

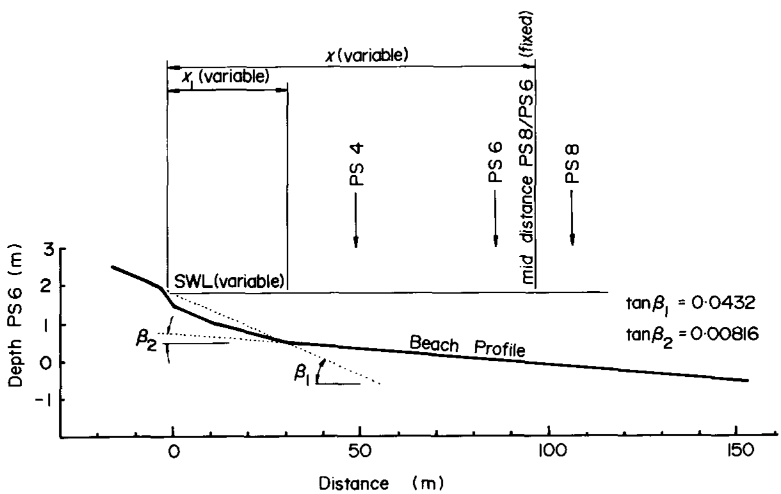

Fig. 8. Beach profile at field site and compound two-slope approximation.

varied as the intersection between still water level and the beach face moved horizontally with changes in tide level.

The results are shown in Table 6. There is close agreement between theory and observation as to the frequencies for which nodes will form between the wave sensing stations, verifying the reliability of Hotta's compound two slope model and its usefulness for predictive purposes. The use of the simple, single slope beach model, adopting a slope biased towards the prevailing flatter slope, produces results which are greatly in error. For example, if an average slope of 0.01 is used and the average observed nodal frequencies of $f_1=0.01$ Hz, $f_2=0.0275$ Hz and $f_3=0.0444$ Hz adopted, then the predicted distance offshore for n_1 (at $L_1/4$), n_2 (at $3L_2/4$) and n_3 (at $5L_3/4$) are all about 30 m or 30% of what they should be. This emphasises the important contribution made to average overall depth on a beach profile by a beach face slope that is steeper than the prevailing offshore slope. For most beaches it is normal for the beach face to be steeper than other parts of the wetted profile. The use of a single slope beach model is then quite unrealistic for the study of surf zone wave reflections at infragravity frequencies.

8. EDGE WAVE CONSIDERATIONS

The preceding work in this paper has shown that the low-frequency surf zone energy exhibits shore-normal water-surface elevation behaviour consistent with that of shore-normal incident waves being reflected and creating two-dimensional onshore–offshore standing waves. The reflection may be partial or total, the degree of reflection seemingly being dependent on frequency and tide level (see Section 4). However, the possibility exists that part of this observed behaviour is attributable to the shore normal standing components of three-dimensional edge waves. The former waves are called leaky mode standing waves where the reflected energy travels back to deep water. There would be no shore-parallel amplitude variations in the sea-surface elevation behaviour. The latter waves are trapped inshore and have shore-parallel as well as shore-normal amplitude variations. Hotta et al. (1981) demonstrated that, at least for a plane beach (single slope), it is difficult to distinguish between these two wave types using only water-surface elevation data from stations aligned in the shore-normal direction, because the node locations are similar. Whether this is valid for a compound two slope beach, as existed at Walker Bay, is debatable.

Studies have shown that total or partial reflection of waves travelling in the shore-normal direction is necessary for the formation and maintenance of three-dimensional edge waves. This has been demonstrated experimentally by Guza and Bowen (1976) and Lin (1987/88). Guza and Bowen also concluded that the edge waves could be suppressed by the high turbulence generated by superimposed broken and breaking waves with frequencies different to that of the two-dimensional standing waves. They further concluded that for edge waves to exist, they must have offshore length scales (decay lengths) that are large in comparison to the surf zone width. The Walker Bay data exhibit the characteristics necessary for this suppression mechanism to exist, with low frequency waves being totally reflected but with higher frequency broken and breaking waves superimposed. Lin (1987/88) concluded that this suppression mechanism had less influence than that attributed by Guza and Bowen.

One point that should be noted, and which has been ignored in the literature, concerns the fact that three-dimensional standing edge waves oscillate in the shore-parallel direction about nodal lines normal to the shore. If a reasonably broad band of edge wave frequencies were present, then the spectra measured simultaneously at three surf zone wave sensors, spaced on a line normal to the shore, should contain some energy troughs at identical frequencies in each spectrum. These would be frequencies for which the instrument line coincided with an edge wave node for shore parallel oscillation. None of the spectra measured at Walker Bay exhibit this characteristic, while they do show energy troughs consistent with two-dimensional standing waves (see Section 3 and Fig. 5). This tends to indicate that either the band of edge wave frequencies present was limited or that any standing edge waves present were very weak. The former hypothesis would, for example, support the Guza and Bowen hypothesis on edge wave suppression.

Another point which tends to diminish the likelihood of significant edge wave presence, relates to the required edge wave modes. The phase shift spectra between stations PS8 and PS6 strongly indicate the existence of nodes at the frequency for which the distance between the effective reflective surface and the wave sensors, matched the distance to the third node for an onshore–offshore standing wave form. The stations PS8 and PS6 were most often less than half the surf zone width seaward of the beach, so that at least 4 or 5 nodes would have been contained within the full surf zone width. Therefore, if part of the observed onshore–offshore structure was attributable to edge waves, then edge waves of mode 4 or 5 or more would have been necessary to produce edge waves with offshore length scales that were large in comparison to the surf zone width, a condition which seems necessary for edge waves to be sustained. Experimental and theoretical investigations have shown that the generation of such high mode edge waves is unlikely, the most likely mode being mode zero (Guza and Inman, 1975; Guza and Bowen, 1976; Chappell and Wright, 1978).

The fact that three-dimensional edge waves may have been present cannot be discounted and any influence they had on the two-dimensional standing wave component cannot be delineated from the data. The evidence does, however, seem to be weighted towards that influence being minimal.

9. CONCLUSIONS

Theoretical considerations and field observations of surf zone water level elevation behaviour in a shore-normal direction, have given rise to the following findings.

(a) A single surf-zone wave height sensor cannot conclusively detect the presence of infragravity shore-normal standing waves, but if they are present, troughs and peaks will occur in the measured spectrum which are not indicative of the energy distribution in the surf zone as whole. The measured spectrum may overestimate or underestimate the general infragravity energy levels contained by the surf zone as a whole, depending on the state of the tide (water depth), the distance from the beach and the range of frequencies over which the infragravity energy is spread. The infragravity peak energy periods determined from a single surf-zone wave height sensor have no real meaning for the surf zone as a whole if shore-normal standing waves are present.

(b) A technique, normally reserved for laboratory applications, has been successfully used on surf-zone field data to separate the true incident and reflected infragravity wave spectra.

(c) The reflection of infragravity waves from a beach was found to be significant for all wave periods greater than 20 s and it can be almost total for wave periods greater than 30 s. The value of the reflection coefficient will vary with tide level. The current study exhibited larger reflection coefficients at higher water levels than at lower water levels with a greater variability in the values observed at low water.

(d) Some quantitative knowledge of the surf-zone infragravity wave activity can be gained by simple observations of the longer-period swash excursions on the beach face. The low-frequency vertical water level motions are about twice those of the incoming long wave phenomenon.

(e) Phase shift spectra from two surf-zone wave height sensors can detect the presence of nodes produced by shore-normal standing waves and provide the data required to compute the frequency associated with those nodes.

(e) The beach face on most beach profiles, tends to be steeper than other parts of the wetted profile. This makes an important contribution to the average depth on the overall profile and makes the use of a simple, single slope beach model quite unrealistic for predicting node location and associated frequencies for shore normal infragravity standing waves. A compound two-slope beach model has been found to yield far more reliable results.

(f) If edge wave activity was present during the experiment, it was either very weak or only spread over a limited band of frequencies.

REFERENCES

Chappell, J. and Wright, L.D., 1978. Surf zone resonance and coupled morphology. Proc. 16th Coastal Engineering Conf., pp. 1359–1377.

Galvin, C.J., 1972. Wave breaking in shallow water. In: R.E. Meyer (Editor), Waves on Beaches. Academic Press, New York, N.Y., pp. 413–456.

Guza, R.T. and Bowen, A.J., 1976. Resonant interactions for breaking waves on a beach. Proc. 15th Coastal Engineering Conf., Vol. 1: 560–579.

Guza, R.T. and Inman, D.L., 1975. Edge waves and beach cusps. J. Geophys. Res., 80(21): 2997–3012.

Hotta, S., Mizuguchi, M. and Isobe, M., 1981. Observations of long period waves in the nearshore zone. Coastal Eng. Jpn, 24: 41–76.

Kinsman, B., 1965. Wind waves, their generation and propagation on the ocean surface. Prentice-Hall, Englewood Cliffs, N.J.

Lin, N.K., 1987/88. Excitation of coastal edge waves. Ocean Phys. Eng., 12: 65–99.

Mansard, E.P.D. and Funke, E.R., 1980. The measurement of incident and reflected spectra using a least squares method. Proc. 17th Coastal Engineering Conf., Vol. 1: 154–172.

Suhayda, J.N. and Pettigrew, N.R., 1977. Observations of wave height and wave celerity in the surf zone. J. Geophys. Res., 82(9): 1419–1424.

Thornton, E.B. and Guza, R.T., 1982. Energy saturation and phase speeds measured on a natural beach. J. Geophys. Res., 87(C12): 9499–9508.

Thornton, E.B., Galvin, J.J., Bub, F.L. and Richardson, D.P., 1976. Kinematics of breaking waves. Proc. 15th Coastal Engineering Conf., Vol. 1: 461–476.

Wright, L.D., Guza, R.T. and Short, A.D., 1982. Dynamics of a high-energy dissipative surf zone. Mar. Geol., 45: 41–62.